

Electroproduction of Charmonia off Nuclei

Yu.P. Ivanov^{a,b,c}, B.Z. Kopeliovich^{b,c,d}, A.V. Tarasov^{b,c,d} and J. Hüfner^{a,b}

^a *Institut für Theoretische Physik der Universität, Philosophenweg 19, 69120 Heidelberg, Germany*

^b *Max-Planck Institut für Kernphysik, Postfach 103980, 69029 Heidelberg, Germany*

^c *Joint Institute for Nuclear Research, Dubna, 141980 Moscow Region, Russia*

^d *Institut für Theoretische Physik der Universität, 93040 Regensburg, Germany*

November 3, 2018

Abstract

In a recent publication we have calculated elastic charmonium production in ep collisions employing realistic charmonia wave functions and dipole cross sections and have found good agreement with the data in a wide range of s and Q^2 . Using the ingredients from those calculations we calculate exclusive electroproduction of charmonia off nuclei. Here new effects become important, (i) color filtering of the $c\bar{c}$ pair on its trajectory through nuclear matter, (ii) dependence on the finite lifetime of the $c\bar{c}$ fluctuation (coherence length) and (iii) gluon shadowing in a nucleus compared to the one in a nucleon. Total coherent and incoherent cross sections for C, Cu and Pb as functions of s and Q^2 are presented together with some differential cross sections. The results can be tested with future electron-nucleus colliders or in peripheral collisions of ultrarelativistic heavy ions.

1 Introduction

In contrast to hadro-production of charmonia, where the elementary production vertex is still debated, electro(photo)production of charmonia seems well understood: the $c\bar{c}$ fluctuation of the incoming real or virtual photon interacts with the target (proton or nucleus) via the dipole cross section $\sigma_{q\bar{q}}$ and the result is projected on the wave function of the observed hadron. In the $\gamma^*p \rightarrow \Psi p$ reaction only the dipole cross section $\sigma_{q\bar{q}}$ and the wave function of the Ψ enter (Ψ stands for J/ψ or ψ'). In comparing calculations with experiment (which fortunately are rather precise and cover a wide range of values s and Q^2 of the incoming γ^*), various parameterizations of the dipole cross section and the wave function have been successfully tested [1]. In the exclusive electroproduction of charmonia $\gamma^*A \rightarrow \Psi X$, where $X = A$ (coherent) or $X = A^*$ (incoherent, where A^* is an excited state of the A -nucleon system) new phenomena are to be expected: color filtering, i.e. inelastic interactions of the $c\bar{c}$ pair on its way through the nucleus is expected to lead to a suppression of Ψ production relative to $A\sigma_{\gamma^*p \rightarrow \Psi p}$. Since the dipole cross section $\sigma_{q\bar{q}}$ also depends on the gluon distribution in the target (p of A), nuclear shadowing of the gluon distribution is expected to reduce $\sigma_{q\bar{q}}$ in a nuclear reaction relative to the one on the proton. Production of a $c\bar{c}$ pair in a nucleus and its absorption are also determined by the values of the coherence length l_c and the formation length l_f .

Explicit calculations have already been performed in [2] in the approximation of a short coherence (or production) length, when one can treat the creation of the colorless $c\bar{c}$ pair as instantaneous,

$$l_c = \frac{2\nu}{M_{c\bar{c}}^2} \approx \frac{2\nu}{M_{J/\psi}^2} \ll R_A, \quad (1)$$

where ν is the energy of the virtual photon in the rest frame of the nucleus. At the same time, the formation length may be long, comparable with the nuclear radius R_A ,

$$l_f = \frac{2\nu}{M_{\psi'}^2 - M_{J/\psi}^2} \sim R_A. \quad (2)$$

In [2] the wave function formation is described by means of the light-cone Green function approach summing up all possible paths of the $c\bar{c}$ in the nucleus. The result has been unexpected. Contrary to naive expectation, based on the larger size of the ψ' compared to J/ψ , it has been found that ψ' is not more strongly absorbed than the J/ψ , but may even be enhanced by the nuclear medium. This is interpreted as an effect of filtering which is easy to understand in the limit of long coherence length, $l_f \gg R_A$, when the ratio of cross sections on nuclear and nucleon targets take the simple form. Indeed, the production rate of ψ' on a proton target is small due to strong cancellations in the projection of the produced $c\bar{c}$ wave packet onto the radial wave function of the ψ' which has a node. After propagation through nuclear matter the transverse size of a $c\bar{c}$ wave packet is squeezed by absorption and the projection of the ψ' wave function is enhanced [2,3] since the effect of the node is reduced.

However, the quantitative predictions of [2] are not trustable since the calculations have been oversimplified and quite some progress has been made on the form of the dipole cross section $\sigma_{q\bar{q}}$ and the light cone wave functions for the charmonia. Therefore we take the problem up again and provide more realistic calculations for nuclear effects in exclusive

electroproduction of charmonia off nuclei relying on the successful parameter free calculations which have been performed recently by the authors [1] for elastic virtual photoproduction of charmonia, $\gamma^* p \rightarrow \Psi p$. Since the present paper is a direct follow up of [1] we do not repeat all definitions and notations, but rather request the reader to consult [1] for more details.

Whenever one deals with high-energy reactions on nuclei, one cannot avoid another problem of great importance: gluon shadowing. At small values of x , gluon clouds overlap in longitudinal direction and may fuse. As a result, the gluon density per one nucleon in a nucleus is expected to be reduced compared to a free proton. Parton shadowing, which leads to an additional nuclear suppression in various hard reactions (DIS, DY, heavy flavor, high- p_T hadrons, etc.) may be especially strong for exclusive vector meson production like charmonium production which needs at least two gluon exchange. Unfortunately, we have no experimental information for gluon shadowing in nuclei so far, and we have to rely on the available theoretical estimates [4–8].

In the present paper we work in the approximation of long coherence time $l_c \gg R_A$ since calculations can be done with great confidence. Only recently [9] the light-cone (LC) dipole approach has been generalized also for the case of a finite coherence length, relevant for the vast majority of available data. However, because of technical difficulties those calculations employ the $\propto r_T^2$ shape of the dipole cross section. It is still a challenge to perform calculations with a realistic dipole cross section for the regime of finite coherence length. Nevertheless, we make corrections for finite values of l_c employing the approximation suggested in [3].

The predictions in this paper are meant as a realistic basis for the planning of future experiments for electron-nucleus collisions at high energies like in the eRHIC project. It would be highly desirable to have good data in order to test the assumptions and ingredients which have entered the calculation and which are important aspects of modern strong interaction many-body physics. Furthermore, progress in the understanding of charmonium electroproduction will also have important consequences for hadroproduction.

The paper is organized as follows. Section 2 introduces some notations and the most important definitions and expressions. Then the integrated cross sections for coherent and incoherent charmonia production are calculated as function of s and Q^2 of the virtual photon and the results are presented as a ratio to A -times the cross sections on a proton. In the following two sections, two important modifications are introduced. The effect of gluon shadowing in the dipole cross section (Section 3) and the case of finite values of l_c ($l_c \simeq R_A$) (Section 4). Appendix A describes some very useful calculational procedures, which considerably increase the accuracy and the speed of numerical calculations.

2 Shadowing and absorption for $c\bar{c}$ pairs in nuclei

Exclusive charmonium production off nuclei, $\gamma^* A \rightarrow \Psi X$ is called coherent, when the nucleus remains intact, i.e. $X = A$, or incoherent, when X is an excited nuclear state which contains nucleons and nuclear fragments but no other hadrons. The cross sections depend on the polarization ϵ of the virtual photon (in all figures below we will imply $\epsilon = 1$),

$$\sigma^{\gamma^* A}(s, Q^2) = \sigma^{\gamma_T^* A}(s, Q^2) + \epsilon \sigma^{\gamma_L^* A}(s, Q^2) , \quad (3)$$

where the indexes T, L correspond to transversely or longitudinally polarized photons, respectively.

The cross section for exclusive production of charmonia off a nucleon target integrated over momentum transfer [10] is given by

$$\sigma_{inc}^{\gamma_{T,L}^* N}(s, Q^2) = \left| \left\langle \Psi \left| \sigma_{q\bar{q}}(r_T, s) \right| \gamma_{c\bar{c}}^{T,L} \right\rangle \right|^2, \quad (4)$$

where $\Psi(\vec{r}_T, \alpha)$ is the charmonium LC wave function which depends on the transverse $c\bar{c}$ separation \vec{r}_T and on the relative sharing α of longitudinal momentum [1]. Both variables are involved in the integration in the matrix element Eq. (4). $\Psi(\vec{r}_T, \alpha)$ is obtained by means of a Lorentz boost applied the solutions of the Schrödinger equation. This procedure involves the Melosh spin rotation [11, 12] which produces sizable effects.

In Eq. (4) $\gamma_{c\bar{c}}^{T,L}(\vec{r}_T, \alpha, Q^2)$ is the LC wave function of the $c\bar{c}$ Fock component of the photon. It depends on the photon virtuality Q^2 . One can find the details in Ref. [1] including the effects of a nonperturbative $q\bar{q}$ interaction.

The cross section $\sigma_{q\bar{q}}(r_T, s)$ describes the interaction of a colorless quark-antiquark dipole of separation r_T and c.m. energy squared s with a nucleon. At small values of r_T the energy dependence should come in the combination $x \sim 1/(r_T^2 s)$ in order to respect Bjorken scaling. A simple parameterization of $\sigma_{q\bar{q}}(r_T, x)$ suggested in [13] (GBW) well describes the data for $F_2^p(x, Q^2)$ at small x and high Q^2 . At low Q^2 , however, the energy variable s is more appropriate. A parameterization for $\sigma_{q\bar{q}}(r_T, s)$ suggested in [6] (KST) describes DIS data only up to $Q^2 \sim 10 \text{ GeV}^2$ which is a scale relevant for charmonia. Since we cannot see why one parameterization should be better than the other, we calculate results for both parameterizations as has been done in [1].

The cross sections for coherent and incoherent production on nuclei will be derived under various conditions imposed by the coherence length Eq. (1). At high energies the coherence length Eq. (1) may substantially exceed the nuclear radius. In this case the transverse size of the $c\bar{c}$ wave packet is “frozen” by Lorentz time dilation, i.e. it does not fluctuate during propagation through the nucleus, and the expressions for the cross sections, incoherent (*inc*) or coherent (*coh*), are particularly simple [2],

$$\sigma_{inc}^{\gamma_{T,L}^* A}(s, Q^2) = \int d^2b T_A(b) \left| \left\langle \Psi \left| \sigma_{q\bar{q}}(r_T, s) \exp \left[-\frac{1}{2} \sigma_{q\bar{q}}(r_T, s) T_A(b) \right] \right| \gamma_{c\bar{c}}^{T,L} \right\rangle \right|^2 \quad (5)$$

$$\sigma_{coh}^{\gamma_{T,L}^* A}(s, Q^2) = \int d^2b \left| \left\langle \Psi \left| 1 - \exp \left[-\frac{1}{2} \sigma_{q\bar{q}}(r_T, s) T_A(b) \right] \right| \gamma_{c\bar{c}}^{T,L} \right\rangle \right|^2. \quad (6)$$

Here $T_A(b) = \int_{-\infty}^{\infty} dz \rho_A(b, z)$ is the nuclear thickness function given by the integral of the nuclear density along the trajectory at a given impact parameter b .

In Eqs. (5) and (6) we also include a small correction due to the real part of the $\gamma^* N \rightarrow \Psi N$ amplitude via replacement

$$\sigma_{q\bar{q}} \Rightarrow \sigma_{q\bar{q}} \left(1 - \frac{i\pi}{2} \frac{\partial \ln \sigma_{q\bar{q}}}{\partial \ln s} \right). \quad (7)$$

As it is common practice we express nuclear cross sections for incoherent and coherent

production in the form of the ratio,

$$R_{\Psi}(s, Q^2) = \frac{\sigma^{\gamma^*A}(s, Q^2)}{A \sigma^{\gamma^*N}(s, Q^2)}, \quad (8)$$

where the numerator stands for the expressions Eqs. (5) and (6) for incoherent and coherent cross sections, respectively. The details of the technically rather complicated numerical calculations of the integrals in Eqs. (5) and (6) can be found in Appendix A.

The ratio Eq. (8) for incoherent electroproduction of J/ψ and ψ' is shown in Fig. 1 as a function of \sqrt{s} . We use the GBW [13] and KST [6] parameterizations for the dipole cross section and show the results by solid and dashed curves, respectively. Differences are at most 10 – 20 %.

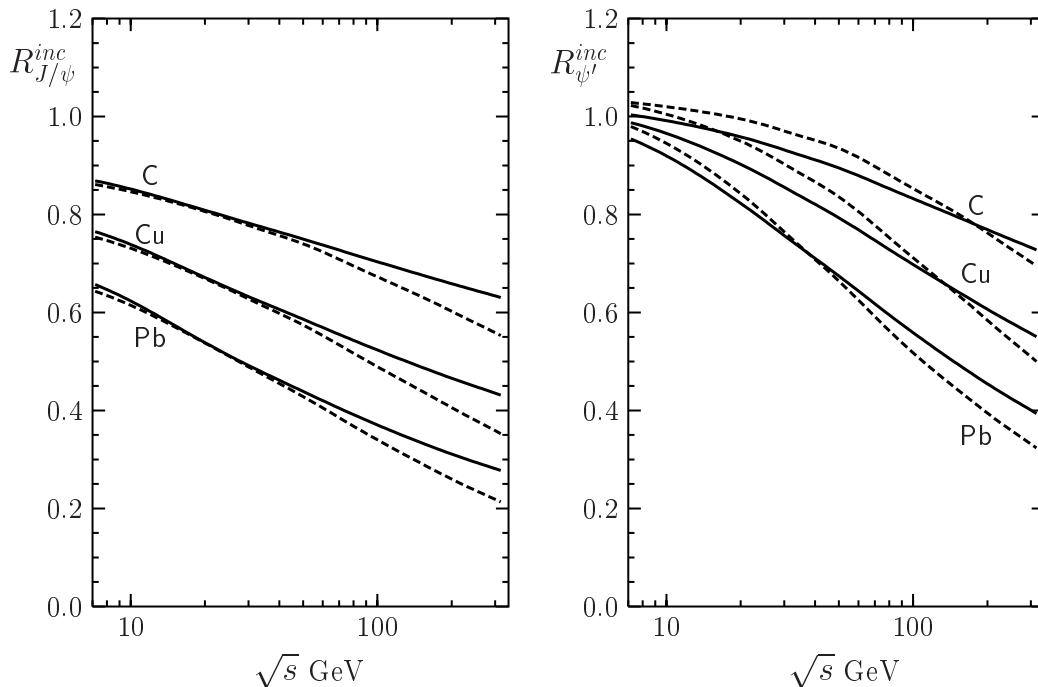


Figure 1: Ratios R_{Ψ}^{inc} for J/ψ and ψ' incoherent production on carbon, copper and lead as function of \sqrt{s} and at $Q^2 = 0$. The solid curves refer to the GBW parameterization of $\sigma_{q\bar{q}}$ and dashed one refer to the KST parameterization.

Analyzing the results shown in Fig. 1, we observe that nuclear suppression of J/ψ production becomes stronger with energy. This is an obvious consequence of the energy dependence of $\sigma_{q\bar{q}}(r_T, s)$, which rises with energy (see in Ref. [1]). For ψ' the suppression is rather similar as for J/ψ . In particular we do not see any considerable nuclear enhancement of ψ' which has been found earlier [2, 14], where the oversimplified form of the dipole cross section, $\sigma_{q\bar{q}}(r_T) \propto r_T^2$ and the oscillator form of the wave function had been used. Such a form of the cross section enhances the compensation between large and small distances in the wave function of ψ' in the process $\gamma^*p \rightarrow \psi'p$. Therefore, the color filtering effect which emphasizes the small distance part of the wave function leads to a strong enhancement of the ψ' production rate. This is why using the more realistic r_T -dependence of $\sigma_{q\bar{q}}(r_T)$ leveling off at large r_T leads to a weaker enhancement of the ψ' . This effect becomes even more pronounced at

higher energies since the dipole cross section saturates starting at a value $r_T \sim r_0(s)$ where $r_0(s)$ decreases with energy. This observation probably explains why the ψ' is less enhanced at higher energies as one can see from Fig. 1.

Note that the “frozen” approximation is valid only for $l_c \gg R_A$ and can be used only at $\sqrt{s} > 20 - 30$ GeV. Therefore, the low-energy part of the curves depicted in Fig. 1 should be corrected for the effects related to the finiteness of l_c . This will be done in Section 4.

One can change the effect of color filtering in nuclei in a controlled way by increasing the photon virtuality Q^2 thereby squeezing the transverse size of the $c\bar{c}$ fluctuation in the photon. For a narrower $c\bar{c}$ pair the cancellation which is caused by the node in the radial wave function of ψ' should be less effective. One expects that the ψ' to J/ψ ratio on a proton target increases with Q^2 , as is observed both in experiment and calculation (Fig. 9 of [1]). Fig. 2 shows the result for nuclear targets: for large values of Q^2 ratios $R_{J/\psi}^{inc}$ and $R_{\psi'}^{inc}$ become very similar. This effect has also been observed in the E665 experiment [15] for exclusive production of ρ and ρ' off nuclei at high energies.

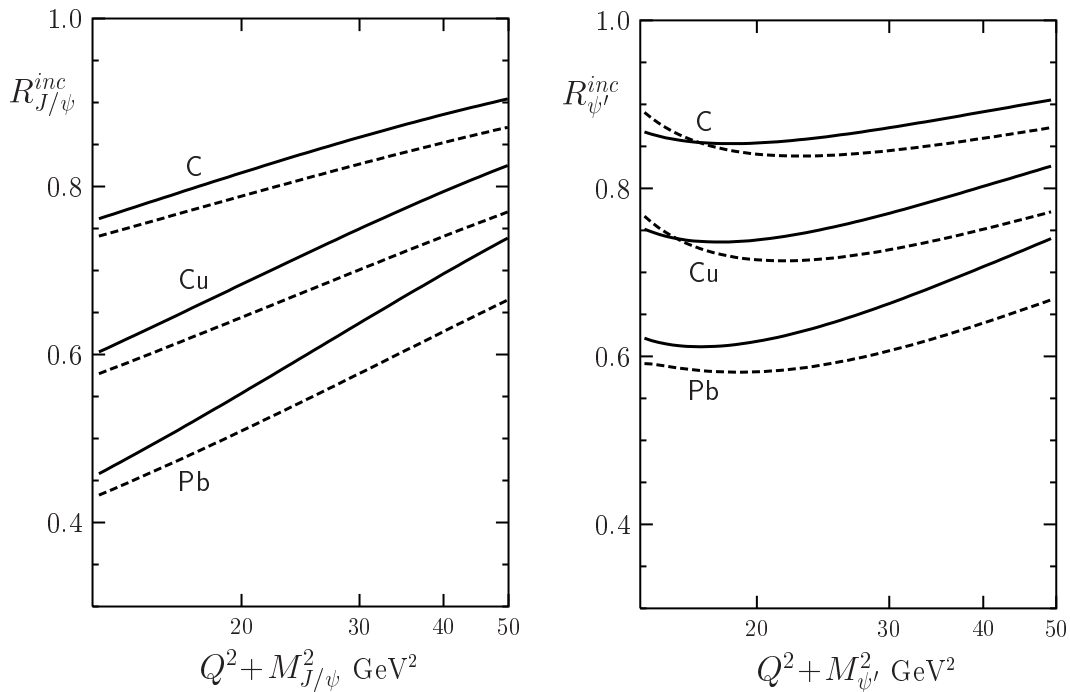


Figure 2: Ratios $R_{J/\psi}^{inc}$ and $R_{\psi'}^{inc}$ for incoherent production on three nuclei displayed as a function of $Q^2 + M_{\Psi}^2$ at fixed $s = 4000$ GeV². The lines are for the GBW (solid curves) and KST (dashed curves) parameterizations.

Nuclear effects for ψ' production shown in Fig. 2 demonstrate an even more peculiar Q^2 dependence. The overlap of the produced $c\bar{c}$ state and the ψ' wave function rises with Q^2 both in the numerator and denominator of the ratio Eq. (8) due to the node effect. However, the nuclear filtering for large size $c\bar{c}$ pairs is especially strong at small Q^2 , hence the Q^2 squeezing does not affect the numerator as much as the denominator. This is why the ratio $R_{\psi'}^{inc}(Q^2)$ can be a falling function at small Q^2 . At high Q^2 , however, the size of the $c\bar{c}$ is so small that color filtering is not an important effect any more, while the nucleus becomes more transparent eventually causing $R_{\psi'}^{inc}(Q^2)$ to rise.

Cross sections for coherent production of charmonia on nuclei are calculated analogously using Eq. (6). The results for the energy dependence are depicted in Fig. 3 and for the Q^2 dependence in Fig. 4. It is not a surprise that the ratios exceed one. In the absence of $c\bar{c}$

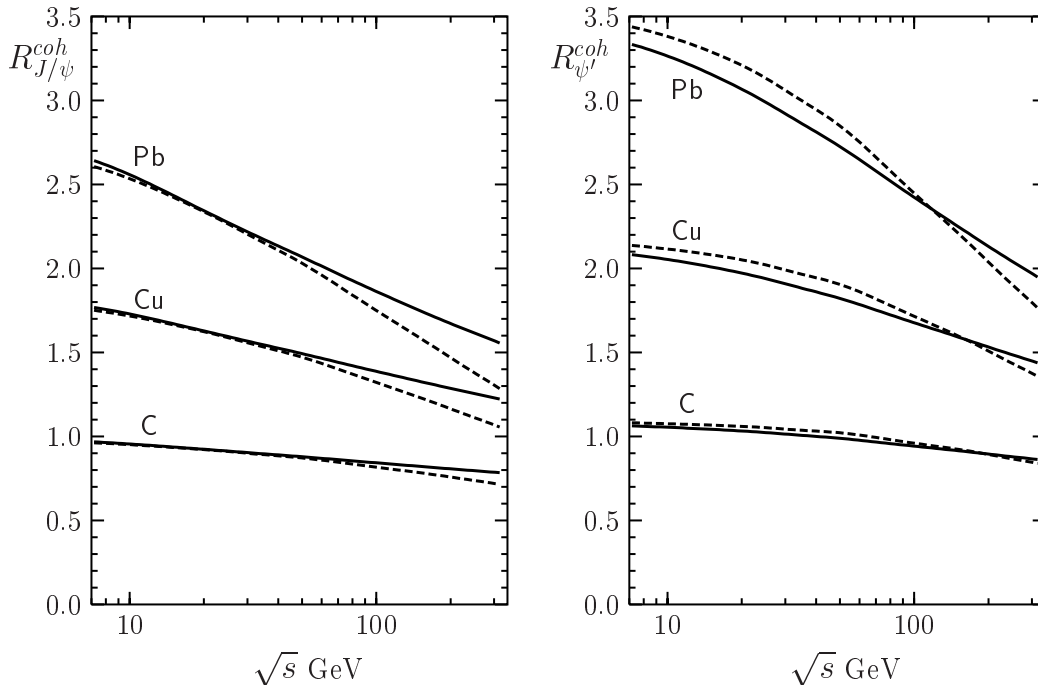


Figure 3: The ratios $R_{J/\psi}^{coh}$ and $R_{\psi'}^{coh}$ for coherent production on nuclei as a function of \sqrt{s} . The meaning of the different lines is the same as in Fig. 1.

attenuation the forward coherent production would be proportional to A^2 , while integrated over momentum transfer, the one depicted in Fig. 3, behaves as $A^{4/3}$. It is a result of our definition Eq. (8) that R_{Ψ}^{coh} exceeds one. To avoid this artifact one may redefine the ratio for coherent processes as,

$$\tilde{R}_{\Psi}^{coh}(s, Q^2) = \frac{\sigma_{coh}^{\gamma^* A}(s, Q^2)}{A \langle T_A \rangle 16\pi B^{\gamma^* N} \sigma^{\gamma^* N}(s, Q^2)} = \frac{R_{\Psi}^{coh}(s, Q^2)}{\langle T_A \rangle 16\pi B^{\gamma^* N}}, \quad (9)$$

where $B^{\gamma^* N}$ is the slope of the $\gamma^* N \rightarrow \Psi N$ differential cross section and

$$\langle T_A \rangle = \frac{1}{A} \int d^2b T_A^2(b) \quad (10)$$

is the mean nuclear thickness. This ratio approaches one when nuclear effects disappear. Nevertheless, we will follow the usual definition Eq. (8) which is widely used for the presentation of data.

We can also predict the dependence on the momentum transfer \vec{k}_T for the charmonium electroproduction on nuclei. In the case of incoherent production this dependence is the same as for production on free nucleons. However, in coherent production the nuclear formfactor comes into play and one has

$$\frac{d\sigma_{coh}^{\gamma_{T,L}^* A}(s, Q^2)}{d^2k_T} = \left| \int d^2b e^{i\vec{k}_T \cdot \vec{b}} \langle \Psi | 1 - \exp \left[-\frac{1}{2} \sigma_{q\bar{q}}(r_T, s) T_A(b) \right] \right| \gamma_{c\bar{c}}^{T,L} \rangle \right|^2. \quad (11)$$

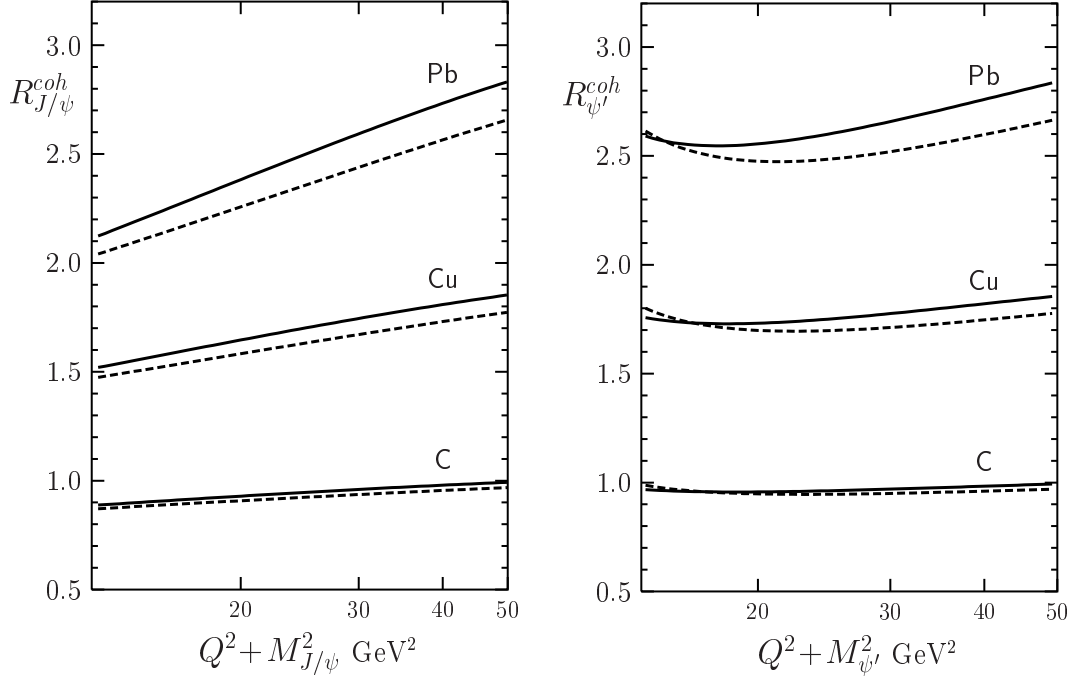


Figure 4: The ratios $R_{J/\psi}^{coh}$ and $R_{\psi'}^{coh}$ for coherent production on various nuclei as a function of Q^2 . The meaning of the lines is the same as in Fig. 2.

In Fig. 5 we plot the ratios of total distributions (sum of T and L components Eq. (11) in the form of Eq. (3) normalized at $Q^2 = 0$ and $k_T = 0$),

$$\mathcal{R}(s, Q^2, k_T) = \frac{d\sigma_{coh}^{\gamma^*A}(s, Q^2)}{d^2k_T} \bigg/ \frac{d\sigma_{coh}^{\gamma^*A}(s, Q^2 = 0)}{d^2k_T} \bigg|_{k_T=0} \quad (12)$$

as functions of k_T at $s = 4000 \text{ GeV}^2$ for different virtualities Q of the photon. We see that the k_T dependences are rather similar for J/ψ and ψ' . The shape of the distribution is governed mainly by the nuclear geometry (and not by the size of the (small) charmonium). The calculated curves show the familiar diffraction pattern known from elastic scattering on nuclei.

3 Gluon shadowing

The gluon density in nuclei at small Bjorken x is expected to be suppressed compared to a free nucleon due to interferences. This phenomenon called gluon shadowing renormalizes the dipole cross section,

$$\sigma_{q\bar{q}}(r_T, x) \Rightarrow \sigma_{q\bar{q}}(r_T, x) R_G(x, Q^2, b). \quad (13)$$

where the factor $R_G(x, Q^2, b)$ is the ratio of the gluon density at x and Q^2 in a nucleon of a nucleus to the gluon density in a free nucleon. No data are available so far which could provide direct information about gluon shadowing. Currently it can be evaluated only theoretically. In what follows we employ the technique developed in [6].

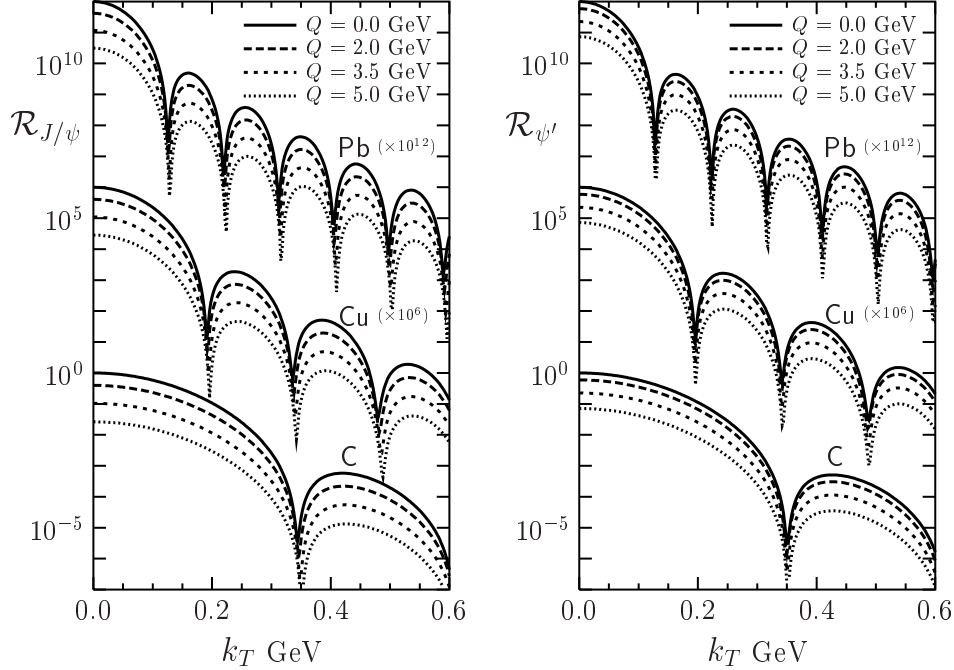


Figure 5: Ratios $\mathcal{R}_{J/\psi}$ and $\mathcal{R}_{\psi'}$ as functions of k_T at $s = 4000 \text{ GeV}^2$ for different values of Q . All curves are calculated with the GBW parameterization of the dipole cross section $\sigma_{q\bar{q}}$.

The interpretation of the phenomenon of gluon shadowing depends very much on the reference frame. It looks like glue-gluon fusion in the infinite momentum frame of the nucleus: although the nucleus is Lorentz contracted, the bound nucleons are still well separated since they contract too. However, the gluon clouds of the nucleons are contracted less since they have a smaller momentum fraction $\sim x$. Therefore, they do overlap and interact at small x , and gluons originating from different nucleons can fuse leading to a reduction of the gluon density.

Although observables must be Lorentz invariant, the space-time interpretation of shadowing looks very different in the rest frame of the nucleus. Here it comes as a result of eikonalization of higher Fock components of the incident particles. Indeed, the nuclear effect included via eikonalization into Eqs. (5)-(6) corresponds to the lowest $c\bar{c}$ Fock component of the photon. These expressions do not include any correction for gluon shadowing, but rather correspond to shadowing of sea quarks in nuclei, analogous to what is measured in deep-inelastic scattering. Although the phenomenological dipole cross section $\sigma_{q\bar{q}}(x, Q^2)$ includes all possible effects of gluon radiation, the eikonal expressions Eqs. (5)-(6) assume that none of the radiated gluons takes part in multiple interaction in the nucleus. The leading order correction corresponding to gluon shadowing comes from eikonalization of the next Fock component which contains the $c\bar{c}$ pair plus a gluon. One can trace on Feynman graphs that this is exactly the same mechanism of gluon shadowing as glue-gluon fusion in a different reference frame.

Note that Eqs. (5)-(6) assume that for the coherence length $l_c \gg R_A$. Even if this condition is satisfied for a $c\bar{c}$ fluctuation, it can be broken for the $c\bar{c}G$ component which is heavier. Indeed, it was found in [16] that the coherence length for gluon shadowing as

about an order of magnitude shorter than the one for shadowing of sea quarks. Therefore, one should not rely on the long coherence length approximation used in (5)-(6), but take into account the finiteness of l_c^G . This can be done by using the light-cone Green function approach developed in [6].

The factor $R_G(x, Q^2, b)$ has the form,

$$R_G(x, Q^2, b) = 1 - \frac{\Delta\sigma(\gamma^*A)}{A\sigma(\gamma^*N)}, \quad (14)$$

where $\sigma(\gamma^*N)$ is the part of the total γ^*N cross section related to a $c\bar{c}$ fluctuation in the photon,

$$\sigma(\gamma^*N) = \int d^2r_T \int_0^1 d\alpha \left| \Psi_{c\bar{c}}^{\gamma^*}(r_T, \alpha, Q^2) \right|^2 \sigma_{q\bar{q}}(r_T, x). \quad (15)$$

Here $\Psi_{c\bar{c}}^{\gamma^*}(r_T, \alpha, Q^2)$ is the light-cone wave function of the $c\bar{c}$ pair with transverse separation \vec{r}_T and relative sharing of the longitudinal momentum α and $1 - \alpha$ (see details in [6]). The numerator $\Delta\sigma(\gamma^*A)$ in (14) reads [6],

$$\begin{aligned} \Delta\sigma(\gamma^*A) &= 8\pi \operatorname{Re} \int d^2b \int dM^2 \left. \frac{d^2\sigma(\gamma^*N \rightarrow c\bar{c}GN)}{dM^2 dq_T^2} \right|_{q_T=0} \\ &\times \int_{-\infty}^{\infty} dz_1 \int_{-\infty}^{\infty} dz_2 \Theta(z_2 - z_1) \rho_A(b, z_1) \rho_A(b, z_2) \exp[-i q_L (z_2 - z_1)]. \end{aligned} \quad (16)$$

Here the invariant mass squared of the $c\bar{c}G$ system reads,

$$M^2 = \sum_i \frac{m_i^2 + k_i^2}{\alpha_i}, \quad (17)$$

where the sum is taken over partons ($c\bar{c}G$) having mass m_i , transverse momentum \vec{k}_i and fraction α_i of the full momentum. The $c\bar{c}G$ system is produced diffractively as an intermediate state in a double interaction in the nucleus. z_1 and z_2 are the longitudinal coordinates of the nucleons N_1 and N_2 , respectively, participating in the diffractive transition $\gamma^* N_1 \rightarrow c\bar{c}G N_1$ and back $c\bar{c}G N_2 \rightarrow \gamma^* N_2$. The value of $\Delta\sigma$ is controlled by the longitudinal momentum transfer

$$q_L = \frac{Q^2 + M^2}{2\nu}, \quad (18)$$

which is related to the gluonic coherence length $l_c^G = 1/q_L$.

The propagation and interaction of the $c\bar{c}G$ system in the nuclear medium between the points z_1 and z_2 is described by the Green function $G_{c\bar{c}G}(\vec{r}_2, \vec{\rho}_2, z_2; \vec{r}_1, \vec{\rho}_1, z_1)$, where $\vec{r}_{1,2}$ and $\vec{\rho}_{1,2}$ are the transverse separations between the c and \bar{c} and between the $c\bar{c}$ pair and gluon at the point z_1 and destination z_2 respectively. Then the Fourier transform of the diffractive cross section in (16)

$$8\pi \int dM_X^2 \left. \frac{d^2\sigma(\gamma^*N \rightarrow XN)}{dM_X^2 dq_T^2} \right|_{q_T=0} \cos[q_L (z_2 - z_1)] \quad (19)$$

can be represented in the form,

$$\begin{aligned} & \frac{1}{2} \text{Re} \int d^2r_2 d^2\rho_2 d^2r_1 d^2\rho_1 \int d\alpha_q d \ln(\alpha_G) \\ & \times F_{\gamma^* \rightarrow c\bar{c}G}^\dagger(\vec{r}_2, \vec{\rho}_2, \alpha_q, \alpha_G) G_{c\bar{c}G}(\vec{r}_2, \vec{\rho}_2, z_2; \vec{r}_1, \vec{\rho}_1, z_1) F_{\gamma^* \rightarrow c\bar{c}G}(\vec{r}_1, \vec{\rho}_1, \alpha_q, \alpha_G) . \end{aligned} \quad (20)$$

Assuming that the momentum fraction taken by the gluon is small, $\alpha \ll 1$, and neglecting the $c\bar{c}$ separation $r \ll \rho$ we arrive at a factorized form of the three-body Green function,

$$G_{c\bar{c}G}(\vec{r}_2, \vec{\rho}_2, z_2; \vec{r}_1, \vec{\rho}_1, z_1) \Rightarrow G_{c\bar{c}}(\vec{r}_2, z_2; \vec{r}_1, z_1) G_{GG}(\vec{\rho}_2, z_2; \vec{\rho}_1, z_1) , \quad (21)$$

where $G_{GG}(\vec{\rho}_2, z_2; \vec{\rho}_1, z_1)$ describes propagation of the GG dipole (in fact the color-octet $c\bar{c}$ and gluon) in the nuclear medium. This Green function satisfies the two dimensional Schrödinger equation which includes the glue-gluon nonperturbative interaction via the light-cone potential $V(\vec{\rho}, z)$, as well as interaction with the nuclear medium.

$$i \frac{d}{dz_2} G_{GG}(\vec{\rho}_2, z_2; \vec{\rho}_1, z_1) = \left[-\frac{\Delta(\vec{\rho}_2)}{2\nu\alpha_G(1-\alpha_G)} + V(\vec{\rho}_2, z_2) \right] G_{GG}(\vec{\rho}_2, z_2; \vec{\rho}_1, z_1) , \quad (22)$$

where

$$2 \text{Im} V(\vec{\rho}, z) = -\sigma_{GG}(\vec{\rho}) \rho_A(b, z) , \quad (23)$$

and the glue-gluon dipole cross section is related to the $q\bar{q}$ one by the relation,

$$\sigma_{GG}(r, x) = \frac{9}{4} \sigma_{q\bar{q}}(r, x) . \quad (24)$$

Following [6] we assume that the real part of the potential has a form

$$\text{Re} V(\vec{\rho}, z) = \frac{b_0^4 \rho^2}{2\nu\alpha_G(1-\alpha_G)} . \quad (25)$$

The parameter $b_0 = 0.65 \text{ GeV}$ was fixed by the data on diffractive gluon radiation (the triple-Pomeron contribution in terms of Regge approach) which is an essential part of Gribov's inelastic shadowing [17]. The well known smallness of such a diffractive cross section explains why b_0 is so large, leading to a rather weak gluon shadowing. In other words, this strong interaction squeezes the glue-gluon wave packet resulting in small nuclear attenuation due to color transparency.

In order to get an analytical solution of Eq. (23) we assume that $\sigma_{GG}(r, s) \approx C_{GG}(s) r^2$, with $C_{GG}(s) = d\sigma_{GG}(r, s)/dr^2|_{r=0}$. We also use the approximation of constant nuclear density $\rho_A(r) = \rho_0 \Theta(R_A - r)$ which is rather accurate for heavy nuclei. Correspondingly $T_A(b) = \rho_0 L(b)$, where $L(b) = 2\sqrt{R_A^2 - b^2}$.

With these simplifications we can perform integration over z_2 in (16) and the gluon shadowing correction takes the form,

$$1 - R_G(x, Q^2) = \rho_0^2 \int \frac{d^2b}{T_A(b)} \int_0^{L(b)} dz (L(b) - z) W(x, Q^2, b, z) , \quad (26)$$

where $W(x, Q^2, b, z)$ reads [6],

$$W(x, Q^2, b, z) = \frac{4\alpha_s(\tilde{Q}^2)}{3\pi C_{q\bar{q}}(x)} \int_x^{x_{\max}} d\alpha_G \frac{C_{GG}^2(\tilde{x}, Q^2, b)}{\alpha_G \tilde{b}^2} \operatorname{Re} \left\{ \exp\left(-\frac{\Omega z}{2t}\right) \times \left[\frac{t}{w} + \frac{\sinh(\Omega z)}{t} \ln\left(1 - \frac{t^2}{u^2}\right) + \frac{2t^3}{uw^2} + \frac{t \sinh(\Omega z)}{w^2} + \frac{4t^3}{w^3} \right] \right\}, \quad (27)$$

$$\alpha_s(Q^2) = \frac{4\pi}{9 \ln \left[(Q^2 + 0.25 \text{ GeV}^2) / \Lambda^2 \right]}, \quad (28)$$

$$\tilde{x} = \min(x/\alpha_G, x_{\max}), \quad (29)$$

$$\tilde{Q}^2 = Q^2 + M_\Psi^2, \quad (30)$$

$$\tilde{b}^2 = \tilde{b}_0^2 + \alpha_G \tilde{Q}^2, \quad (31)$$

$$B = \sqrt{\tilde{b}^4 - i\alpha_G(1-\alpha_G)\nu\rho_0 C_{GG}(\tilde{x}, b)}, \quad (32)$$

$$\Omega = iB / (\alpha_G(1-\alpha_G)\nu), \quad (33)$$

$$t = B / \tilde{b}^2, \quad (34)$$

$$u = t \cosh(\Omega z) + \sinh(\Omega z), \quad (35)$$

$$w = (1 + t^2) \sinh(\Omega z) + 2t \cosh(\Omega z). \quad (36)$$

Here $x_{\max} = 0.1$ and $\Lambda = 200$ MeV. The factor $C_{GG}(x, Q^2, b)$ is determined by the condition of equivalent descriptions in the limit $l_c^G \gg R_A$ using the realistic parameterization for $\sigma_{GG}(r_T)$ and its simplified form $\sigma_{GG}(r_T) = C_{GG} r_T^2$,

$$\left\langle\left\langle C_{GG}(x, Q^2, b) r_T^2 T_A(b) \right\rangle\right\rangle = \left\langle\left\langle \frac{9}{4} \sigma_{q\bar{q}}(x, r_T) R_G(x, Q^2, b) T_A(b) \right\rangle\right\rangle. \quad (37)$$

Here

$$\left\langle\left\langle f(r_T) \right\rangle\right\rangle \equiv \frac{\int d^2\vec{r}_T |\Psi_{qG}(r_T)|_{\text{eff}}^2 \left(1 - e^{-\frac{1}{2}f(r_T)}\right)}{\int d^2\vec{r}_T |\Psi_{qG}(r_T)|_{\text{eff}}^2 f(r_T)}, \quad (38)$$

and the nonperturbative light-cone wave function of the GG (in fact $c\bar{c}$ and G) dipole,

$$|\Psi_{GG}(r_T)|_{\text{eff}}^2 \propto \frac{e^{-b_0^2 r_T^2}}{r_T^2}. \quad (39)$$

Obtaining the gluon shadowing factor $R_G(b)$ one can relate it to the corresponding value $T_A(b)$. This gives R_G as a function of thickness T_A , $R_G(T_A)$. This function is then used in calculations where $T_A(b)$ is obtained with the realistic Woods-Saxon nucleus density.

Fig. 6 shows the ratios of cross sections calculated with and without gluon shadowing

$$S_G(s, Q^2) = \frac{\sigma_G^{\gamma^*A}(s, Q^2)}{\sigma^{\gamma^*A}(s, Q^2)} \quad (40)$$

for incoherent and coherent exclusive charmonium electroproduction. We see that the onset of gluon shadowing happens at a c.m. energy of few tens GeV. This is controlled by the

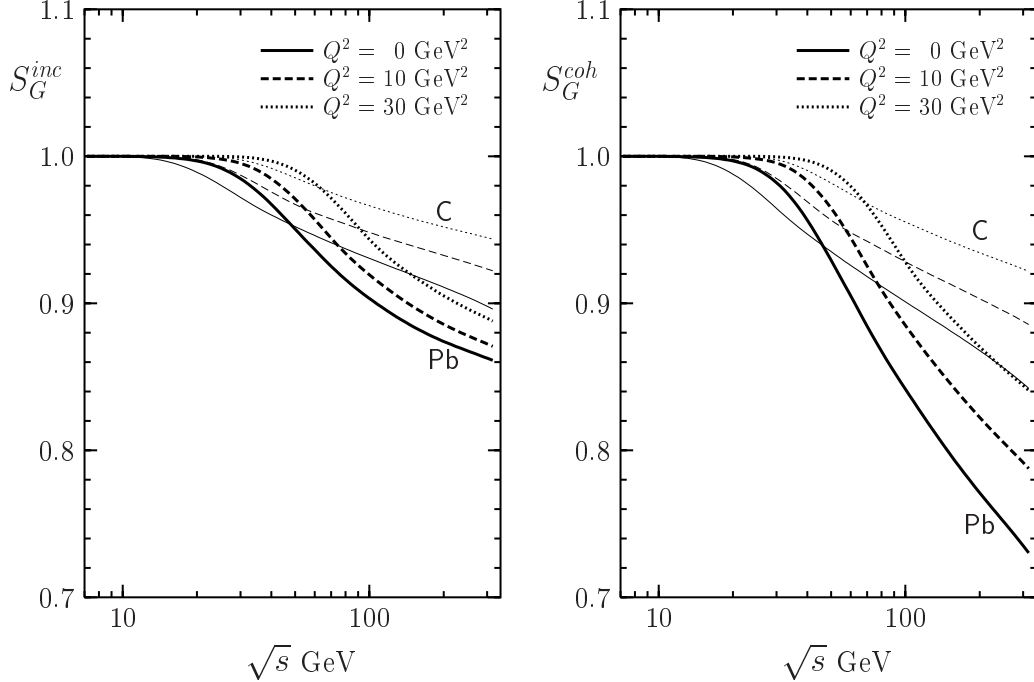


Figure 6: Ratios $S_G(s, Q^2)$ of cross sections calculated with and without gluon shadowing for incoherent and coherent charmonia production. We only plot ratios for J/ψ production, because ratios for ψ' production are practically the same. All curves are calculated with the GBW parameterization of the dipole cross section $\sigma_{q\bar{q}}$.

nuclear formfactor which depends on the longitudinal momentum transfer $q_c = 1/l_c^G$. It was found in [16] that the coherence length for gluon shadowing is rather short,

$$l_c^G \approx \frac{1}{10 x m_N}, \quad (41)$$

where x in our case should be an effective one, $x = (Q^2 + M_\Psi^2)/2\nu$. The onset of shadowing should be expected at $q_c^2 \sim 3/(R_A^{ch})^2$ corresponding to

$$s_G \sim 10 m_N R_A^{ch} (Q^2 + M_\Psi^2) / \sqrt{3}, \quad (42)$$

where $(R_A^{ch})^2$ is the mean square of the nuclear charge radius. This estimate is in a good agreement with Fig. 6. Remarkably, the onset of shadowing is delayed with rising nuclear radius and Q^2 .

Fig. 7 shows the effect of shadowing for the k_T dependence of the coherent photoproduction. As one can see these corrections are quite small for $Q^2 = 0$ (and even smaller with increasing Q^2 , see Eqs. (26) and (27)).

4 Finite coherence length.

A strictly quantum-mechanical treatment of a fluctuating $q\bar{q}$ pair propagating through an absorptive medium based on the LC Green function approach has been suggested recently

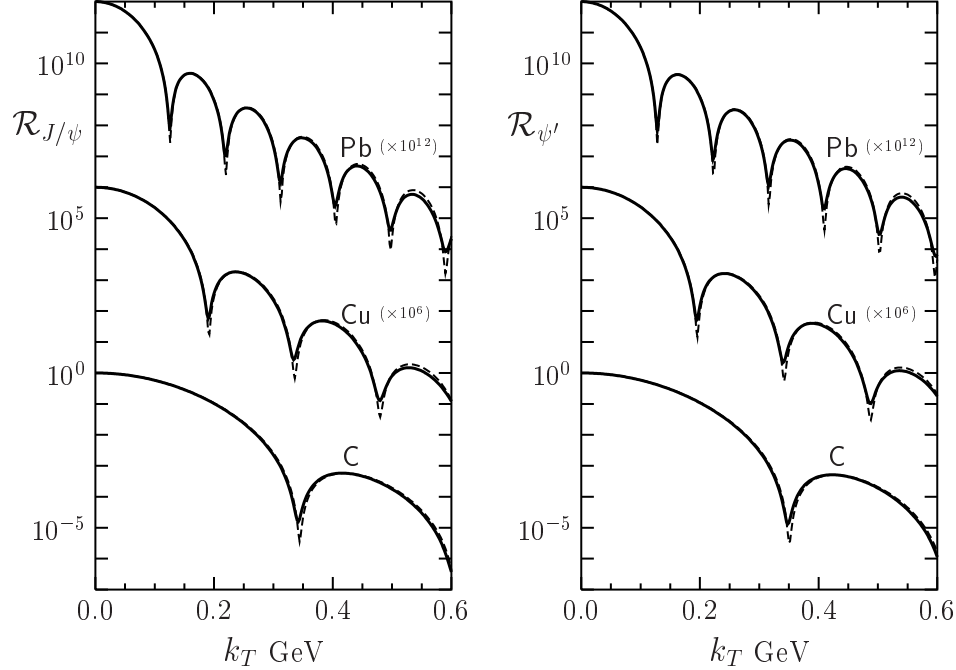


Figure 7: Ratio \mathcal{R}_Ψ as a function of k_T at $s = 4000 \text{ GeV}^2$ and $Q^2 = 0$ with gluon shadowing (solid curves) and without (dashed curves) with the GBW parameterization of the dipole cross section.

in [9]. However, an analytical solution for the LC Green function is known only for the simplest form of the dipole cross section $\sigma_{q\bar{q}}(r_T) \propto r_T^2$. With a realistic form of $\sigma_{q\bar{q}}(r_T)$ it is possible only to solve this problem numerically, what is still a challenge. Here we use the approximation suggested in [18] to evaluate the corrections arising from the finiteness of $l_c = 2\nu/M_\Psi^2$ by multiplying the cross sections for incoherent and coherent production evaluated for $l_c \rightarrow \infty$ by a kind of formfactor F^{inc} and F^{coh} respectively:

$$\sigma^{\gamma A \rightarrow \Psi X}(s, Q^2) \Rightarrow \sigma^{\gamma A \rightarrow \Psi X}(s, Q^2) \cdot F^{inc}(s, l_c(s, Q^2)) , \quad (43)$$

$$\sigma^{\gamma A \rightarrow \Psi A}(s, Q^2) \Rightarrow \sigma^{\gamma A \rightarrow \Psi A}(s, Q^2) \cdot F^{coh}(s, l_c(s, Q^2)) , \quad (44)$$

where

$$F^{inc}(s, l_c) = \int d^2\mathbf{b} \int_{-\infty}^{\infty} dz \rho_A(\mathbf{b}, z) |F_1(s, \mathbf{b}, z) - F_2(s, \mathbf{b}, z, l_c)|^2 / (\dots)|_{l_c=\infty} , \quad (45)$$

$$F^{coh}(s, l_c) = \int d^2\mathbf{b} \left| \int_{-\infty}^{\infty} dz \rho_A(\mathbf{b}, z) F_1(s, \mathbf{b}, z) e^{iz/l_c} \right|^2 / (\dots)|_{l_c=\infty} , \quad (46)$$

$$F_1(s, \mathbf{b}, z) = \exp\left(-\frac{1}{2} \sigma_{\Psi N}(s) \int_z^\infty dz' \rho_A(\mathbf{b}, z')\right) , \quad (47)$$

$$F_2(s, \mathbf{b}, z, l_c) = \frac{1}{2} \sigma_{\Psi N}(s) \int_{-\infty}^z dz' \rho_A(\mathbf{b}, z') F_1(\mathbf{b}, z') e^{-i(z-z')/l_c} . \quad (48)$$

For the charmonium nucleon total cross section $\sigma_{\Psi N}(s)$ we use our previous results [1], essentially the expectation value of the dipole cross section $\sigma_{q\bar{q}}(r_T, s)$ taken between the LC wave functions for the charmonia. The “formfactors” F^{inc} for incoherent J/ψ and ψ' production are depicted in Fig. 8. The observed nontrivial energy dependence is easy to

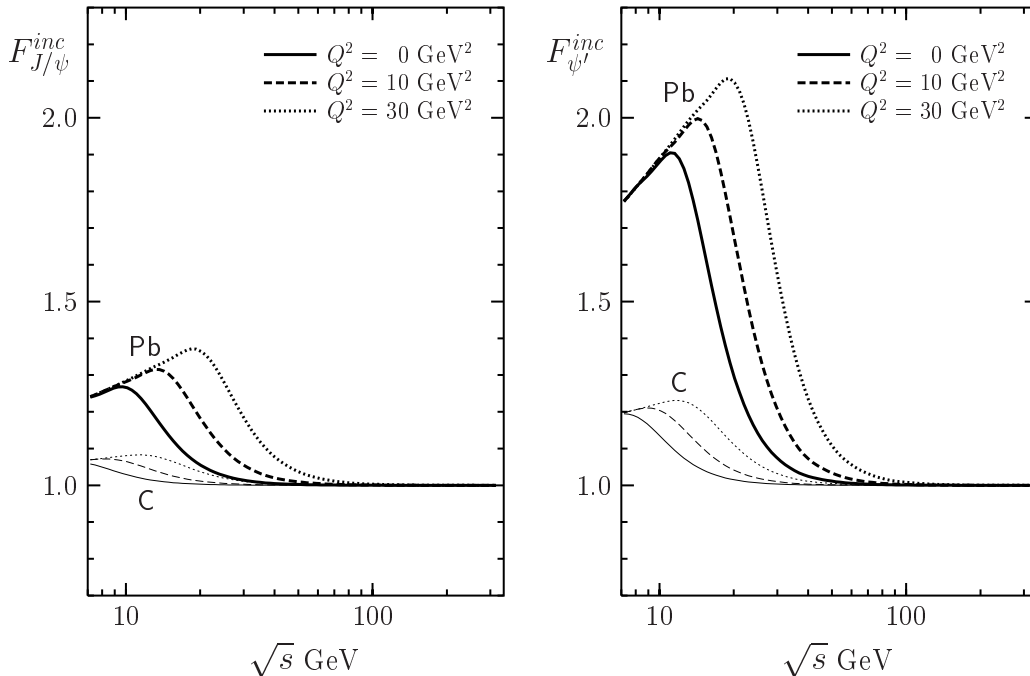


Figure 8: l_c corrections for incoherent production of J/ψ and ψ' on C (thin curves) and Pb (thick curves) for the GBW parameterization of the dipole cross section $\sigma_{q\bar{q}}$.

interpret. At low energies $l_c \ll R_A$ and the photon propagates without any attenuation inside the nucleus where it develops for a short time t_c a $c\bar{c}$ fluctuation which momentarily interacts to get on mass shell. The produced $c\bar{c}$ pair attenuates along the path whose length is a half of the nuclear thickness on the average. On the other hand, at high energies $l_c \gg R_A$ and the $c\bar{c}$ fluctuation is developed long before its interaction with the nucleus. As a result, it propagates through the whole nucleus and the mean path length is twice as long as at low energies. This is why the nuclear transparency drops when going from the regimes of short to long l_c .

One can simplify expression (45) assuming $\sigma_{\Psi N} T_A(b) \ll 1$ which is a rather accurate approximation for J/ψ . Then one can expand the exponentials in (47)-(48) and obtain [3],

$$F_{J/\psi}^{inc}(s) = \frac{1 - \frac{1}{2} [1 + F_A^2(q_c)] \sigma_{J/\psi N}(s) \langle T_A \rangle}{1 - \sigma_{J/\psi N}(s) \langle T_A \rangle}. \quad (49)$$

Here

$$F_A^2(q) = \frac{1}{\langle T_A \rangle} \int d^2b \left| \int_{-\infty}^{\infty} dz \rho_A(b, z) e^{iqz} \right|^2 \quad (50)$$

is the so called longitudinal nuclear formfactor.

At low energies, $q_c \equiv 1/l_c \gg 1/R_A$, the formfactor $F_A^2(q_c) = 0$ and both the numerator and denominator in (49) decrease with energy due to the rising $\sigma_{J/\psi N}(s)$, but the denominator does it faster. This is why the ratio Eq. (49) rises with energy unless it drops due to the rise of the formfactor $F_A^2(q_c) \neq 0$. The transition energy regime is related to the variation of the formfactor between 0 and 1, i.e. at

$$s_{c\bar{c}} \sim m_N(M_{J/\psi}^2 + Q^2)R_A^{ch}/\sqrt{3} = \frac{1}{10}s_G . \quad (51)$$

This energy increases with Q^2 and nuclear radius in accordance with Fig. 8.

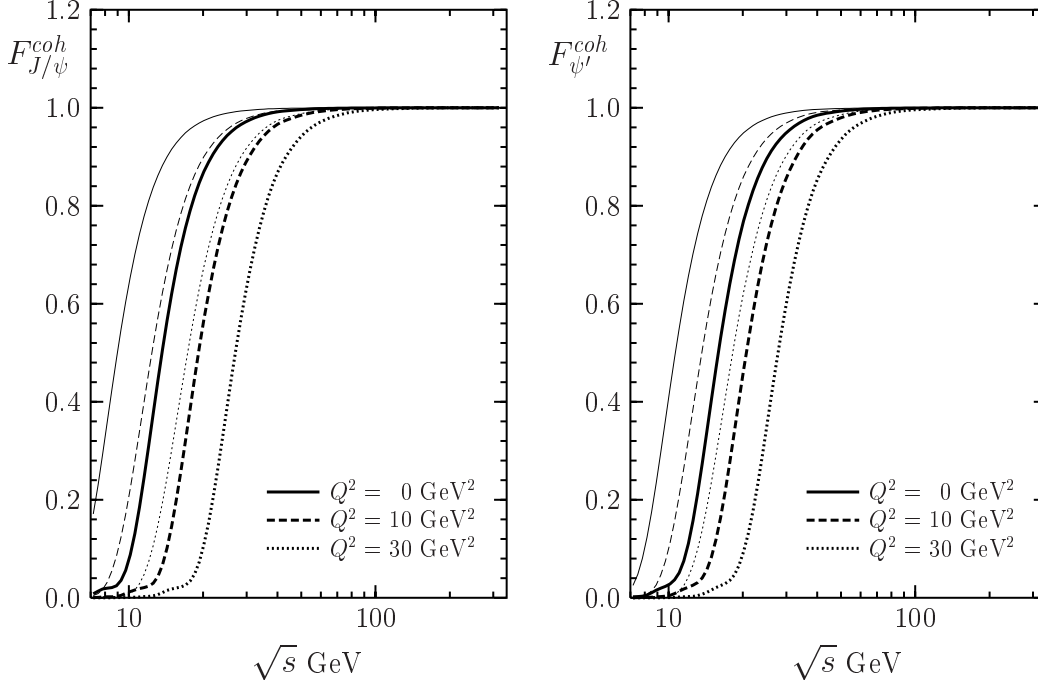


Figure 9: l_c corrections for coherent production of J/ψ and ψ' on C (thin curves) and Pb (thick curves) for the GBW parameterization of the dipole cross section. Contrary to the case of incoherent production results for J/ψ and ψ' are very similar.

Note that the Glauber approximation used to calculate F^{inc} is rather good for J/ψ , but not for ψ' . One could improve it applying the rigorous description based on the light-cone Green function formalism developed in [9] for exclusive production of vector mesons. However, it was done only for the unrealistic form of the dipole cross sections $\sigma_{q\bar{q}} \propto r_T^2$ and for an oscillatory wave function of the vector meson. It is still a challenge to make this approach realistic.

The results for the energy dependence of the formfactor F^{coh} for coherent scattering are shown on Fig. 9. In the limit of low energies $l_c \rightarrow 0$ the strongly oscillating exponential phase factor in (46) makes the integral very small and thus $F_{J/\psi}^{coh} \approx 0$. Then the cross section rises with l_c unless it saturates at $l_c \gg R_A$ when the phase factor becomes constant. Apparently, this transition region is shifted to higher energies for larger Q^2 and nuclear radius as is confirmed by the curves in Fig. 9.

5 Final results and conclusions

Combining the results of the previous sections (i.e. including finite coherence length and gluon shadowing) we obtain the final results for ratios the $R_{J/\psi}$ and $R_{\psi'}$. Figs. 10 and 11 show the s and Q^2 dependences for incoherent and Figs. 12 and 13 for coherent production of charmonia.

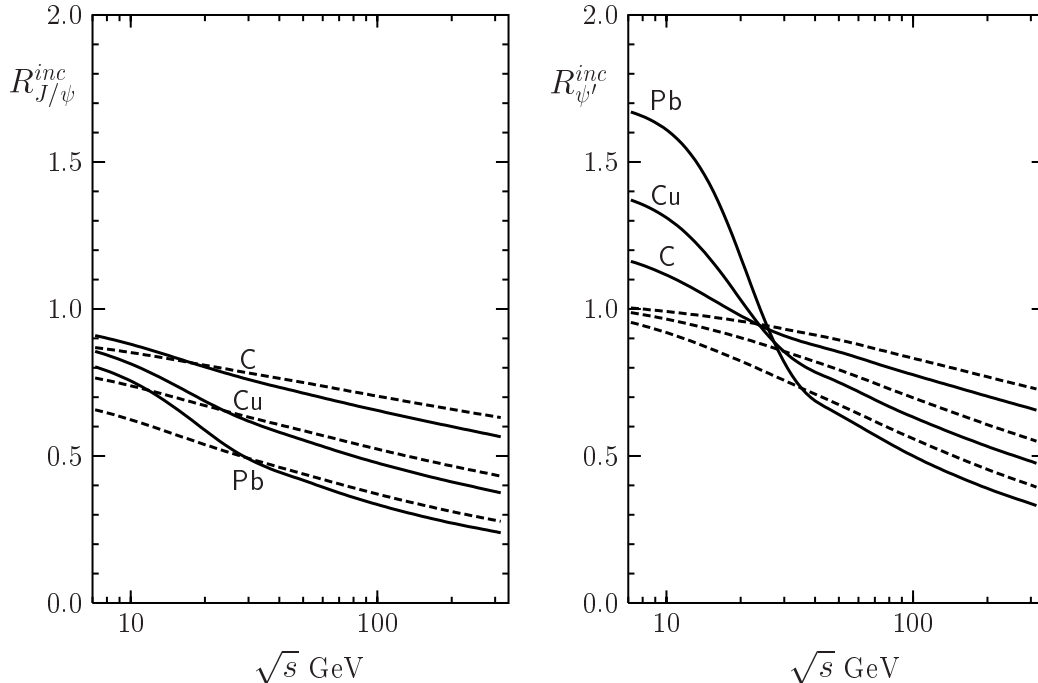


Figure 10: Ratios R_{Ψ}^{inc} for J/ψ and ψ' incoherent production on carbon, copper and lead as function of \sqrt{s} and at $Q^2 = 0$ calculated with GBW parameterization of $\sigma_{q\bar{q}}$. Solid curves display the modifications due to the gluon shadowing and finite coherence length l_c while the dashed lines are without (same as on Fig. 1).

We summarize, in this paper we provide predictions for nuclear effects in exclusive electroproduction of charmonia on nuclei with realistic light-cone wave functions of charmonia and with dipole cross sections which have been already tested in a calculation of elastic charmonium electroproduction off protons. Such calculations still can be performed only at rather high energies where the coherence length exceeds the nuclear size ($l_c \gg R_A$). At these energies gluon shadowing which is absent at lower energies ($l_c \sim R_A$) becomes an important and sometimes the dominant effect. Since no reliable experimental information about gluon shadowing is available so far, we have performed calculations of this effect employing the same light-cone dipole approach. We found sizable, but not large corrections (10-20%) which, however, keep rising with energy. It turns out that the magnitude of gluon shadowing is suppressed by a nonperturbative interaction of the light-cone gluons which is well fixed by data on large mass diffraction. The effects related to finiteness of the coherence length at somewhat lower energies were estimated too.

We have calculated both coherent and incoherent cross sections as function of energy, Q^2 and momentum transfer. Our predictions can be tested in future experiments at high

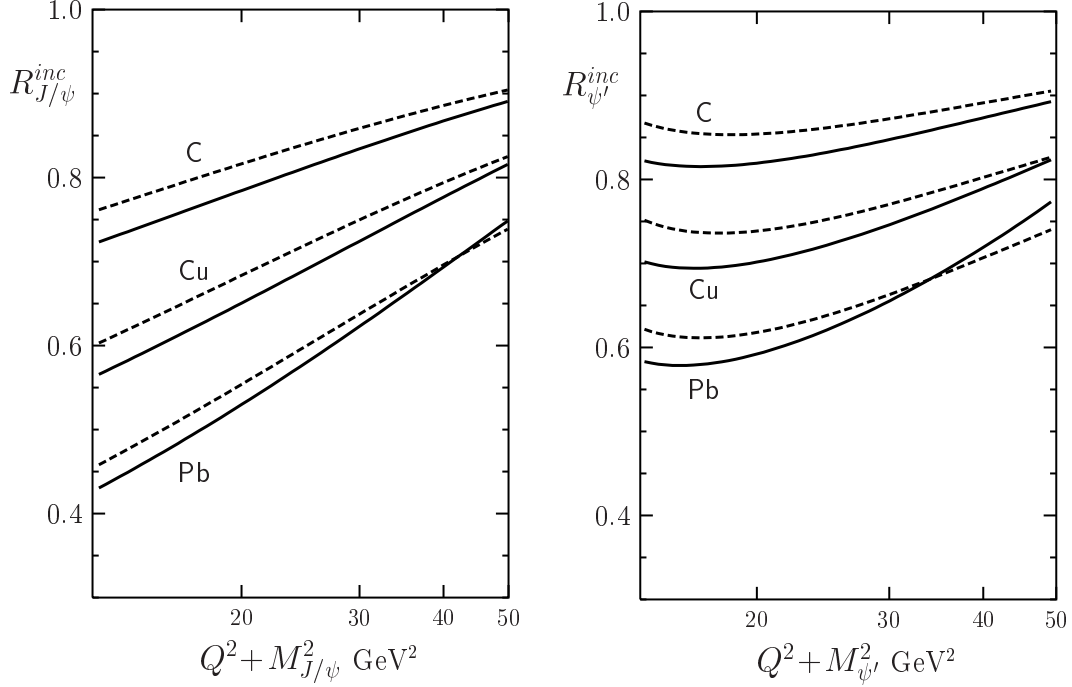


Figure 11: Ratios R_{Ψ}^{inc} for J/ψ and ψ' incoherent production on carbon, copper and lead as function of $Q^2 + M_{\Psi}^2$ at fixed $s = 4000 \text{ GeV}^2$ for GBW parameterization of the dipole cross section $\sigma_{q\bar{q}}$. Solid curves correspond to the final result (with gluon shadowing and l_c corrections) while thin curves are without (same as on Fig. 2).

energies with electron-nuclear colliders (eRHIC). It also can be produced in peripheral heavy ion collisions (RHIC, LHC), and our predictions will be published elsewhere.

Acknowledgment: The authors gratefully acknowledge the partial support by a grant from the Gesellschaft für Schwerionenforschung Darmstadt (grant no. GSI-OR-SCH) and by the Federal Ministry BMBF (grant no. 06 HD 954). We are grateful to Jan Nemchik who read the manuscript and made many valuable comments.

Appendix A Resummation expressions

Matrix elements of the dipole cross section $\sigma_{q\bar{q}}$ for the charmonia production including the effects of spin rotation were calculated in [1] for the specific form of the r_T dependence provided by the KST and GBW parameterizations:

$$\sigma_{q\bar{q}}(r_T) = \sigma_0 \left[1 - \exp\left(-\frac{r_T^2}{r_0^2}\right) \right]. \quad (\text{A.1})$$

In the nuclear case one needs to calculate matrix elements of the operators with $\sigma_{q\bar{q}}$ in the exponent. For incoherent and coherent scattering one can use Taylor expansion, for example:

$$\langle \sigma e^{-c\sigma} \rangle = \left\langle \sigma - c\sigma^2 + \frac{c^2\sigma^3}{2} + \dots \right\rangle = \langle \sigma \rangle \cdot \left(1 - cf_1 + \frac{c^2 f_2}{2} + \dots \right), \quad (\text{A.2})$$

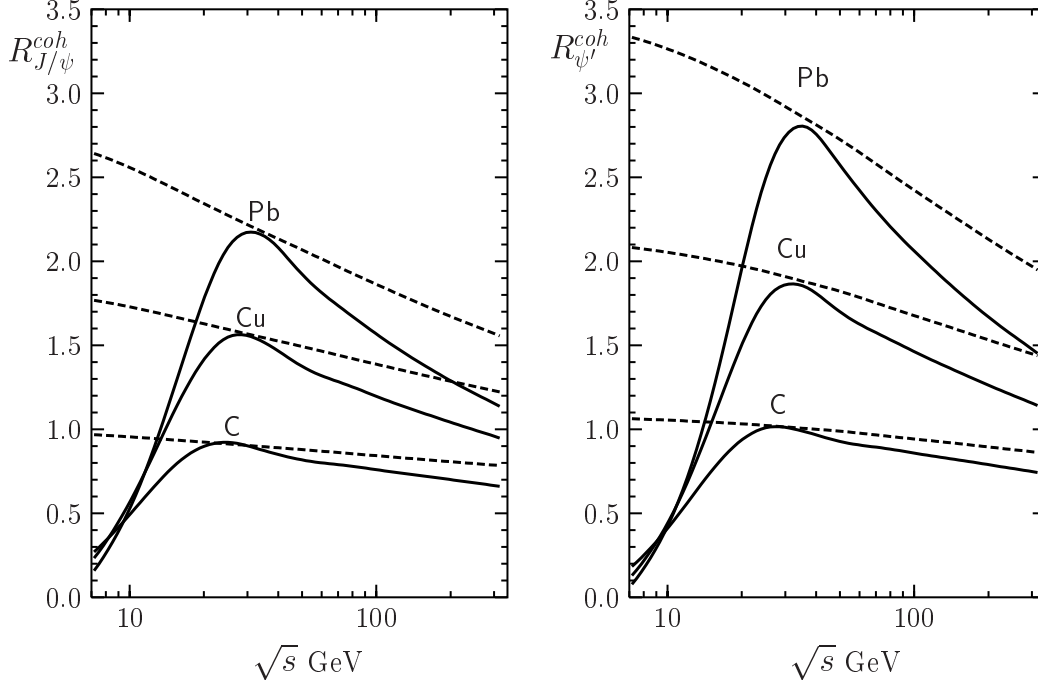


Figure 12: Ratios $R_{J/\psi}^{coh}$ and $R_{\psi'}^{coh}$ for coherent production on nuclei as a function of \sqrt{s} . The meaning of the different lines is the same as in Fig. 10. Thin curves correspond to Fig. 3.

$$\langle 1 - e^{-c\sigma} \rangle = \left\langle c\sigma - \frac{c^2\sigma^2}{2} + \frac{c^3\sigma^3}{6} + \dots \right\rangle = c \langle \sigma \rangle \cdot \left(1 - \frac{cf_1}{2} + \frac{c^2f_2}{6} + \dots \right), \quad (\text{A.3})$$

where $f_n \equiv \langle \sigma^{n+1} \rangle / \langle \sigma \rangle$ and c doesn't depend on initial and final states. So matrix elements of powers $\sigma_{q\bar{q}}^n$ have to be calculated. The form (A.1) allows to express any power of $\sigma_{q\bar{q}}(r_T)$ as a sum of exponentials $\exp(-r_T^2/r_0^2)$ with reduced $r_0^2 \Rightarrow r_0^2/m$, i.e. $\langle \sigma^n \rangle$ can be expressed in terms of $\langle \sigma \rangle$ with reduced r_0^2 .

The rate of convergence of such series slows down with increasing σ (larger s) and increasing nuclear thickness ($c \propto T_A(b)$). In our calculations we used a more efficient expansion, which contains matrix elements $\langle \sigma^n \rangle$ in the exponent. This form can be obtained when applying the identity

$$1 + x = e^{\log(1+x)} = \exp\left(x - \frac{x^2}{2} + \frac{x^3}{3} + \dots\right) \quad (\text{A.4})$$

to (A.2) (with $x = cf_1 + \dots$) and (A.3) (with $x = -cf_1/2 + \dots$). As a result one can get

$$\langle \sigma e^{-c\sigma} \rangle = \langle \sigma \rangle \cdot \exp\left(-cf_1 + \frac{c^2}{2}(f_2 - f_1^2) + \dots\right), \quad (\text{A.5})$$

$$\langle 1 - e^{-c\sigma} \rangle = c \langle \sigma \rangle \cdot \exp\left(-\frac{cf_1}{2} + c^2\left(\frac{f_2}{6} - \frac{f_1^2}{8}\right) + \dots\right), \quad (\text{A.6})$$

which converges noticeable faster. Fig. 14 shows that while one needs about six terms ($n = 6$) to obtain an accurate result using Taylor expansion (A.2), one has already satisfactory results for $n = 2$ in the method, where one resums in the exponent.

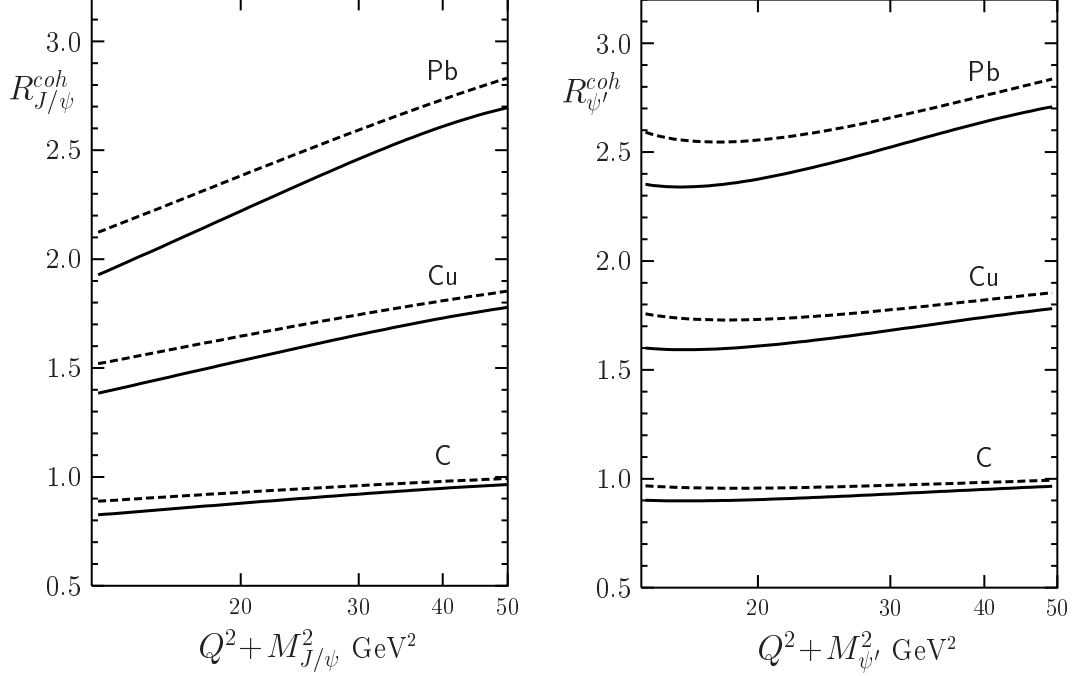


Figure 13: Ratios R_{Ψ}^{inc} for J/ψ and ψ' coherent production on carbon, copper and lead as function of $Q^2 + M_{\Psi}^2$ at fixed $s = 4000 \text{ GeV}^2$ for GBW parameterization of the dipole cross section $\sigma_{q\bar{q}}$. The meaning of the different lines is the same as in Fig. 11. Thin curves correspond to Fig. 4.

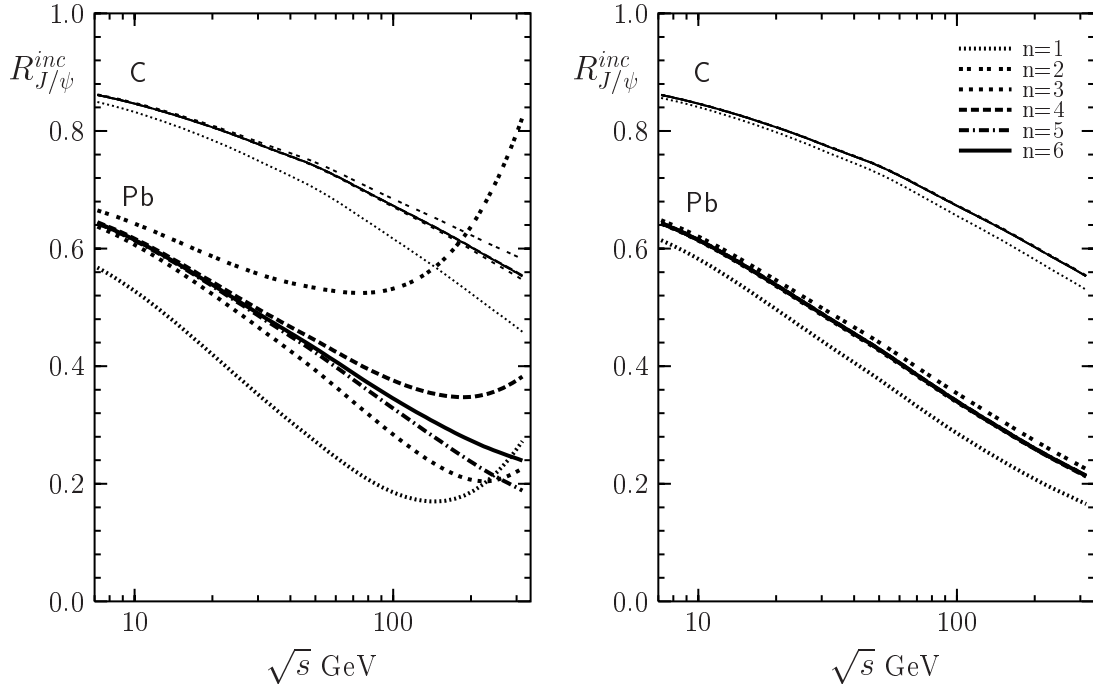


Figure 14: Convergence of the series (A.2) (left) and resummation in the exponent (A.5) (right) for incoherent J/ψ production on nuclei ($Q^2 = 0$, gluon shadowing and l_c corrections are not included) for different orders of summation on f_n .

References

- [1] J. Huefner *et al.*, Phys. Rev. D **62**, 094022 (2000); hep-ph/0007111.
- [2] B.Z. Kopeliovich and B.G. Zakharov, Phys. Rev. D **44**, 3466 (1991).
- [3] O. Benhar *et al.*, Phys. Rev. Lett. **69**, 1156 (1992).
- [4] A.H. Mueller, Nucl. Phys. B **335**, 115 (1990).
- [5] Nucl. Phys. B **558**, 285 (1999); hep-ph/9904404.
- [6] B.Z. Kopeliovich, A. Schäfer and A.V. Tarasov, Phys. Rev. D **62** 0540022; hep-ph/9908245.
- [7] B.Z. Kopeliovich *et al.*, hep-ph/0110221.
- [8] B. Blättel *et al.*, Phys. Rev. Lett. **71**, 896 (1993).
- [9] B.Z. Kopeliovich *et al.*, Phys. Rev. C **65**, 035201 (2002); hep-ph/0107227.
- [10] A.B. Zamolodchikov, B.Z. Kopeliovich and L.I. Lapidus, Sov. Phys. JETP Lett. **3**, 595 (1981) [Pis'ma Zh. Eksp. Teor. Fiz. **33**, 612 (1981)].
- [11] M.V. Terent'ev, Yad. Fiz. **24** 53 (1976) [Sov. J. Nucl. Phys. **24** 106 (1976)].
- [12] H.J. Melosh, Phys. Rev. D **9**, 1095 (1974); W. Jaus, Phys. Rev. D **41**, 3394 (1990).
- [13] K. Golec-Biernat and M. Wüsthoff, Phys. Rev. D **53**, 014017 (1999); hep-ph/9903358.
- [14] B.Z. Kopeliovich *et al.*, Phys. Lett. B **324**, 469 (1994).
- [15] E665 Collaboration, M.R. Adams *et al.*, Phys. Rev. Lett. **74**, 1525 (1995).
- [16] B.Z. Kopeliovich, J. Raufeisen, A.V. Tarasov, Phys. Rev. C **62**, 035204 (2000).
- [17] V.N. Gribov, Sov. Phys. JETP **29**, 483 (1969) [Zh. Eksp. Teor. Fiz. **56**, 892 (1969)].
- [18] J. Hüfner, B.Z. Kopeliovich and A.B. Zamolodchikov, Z. Phys. A **357**, 113 (1997).